Full-length Rat Amylin Forms Fibrils Following Substitution of Single Residues from Human Amylin

Janelle Green[1], Claire Goldsbury[2], Thierry Mini[3], Shabir Sunderji[4] Peter Frey[4], Joerg Kistler[5], Garth Cooper[5,6] and Ueli Aebi[1]*

[1]*M.E. Müller-Institute for Structural Biology, Biozentrum University of Basel Klingelbergstrasse 70, 4056 Basel, Switzerland*

[2]*Max-Planck Unit for Structural Molecular Biology Notkestrasse 85, 22607 Hamburg, Germany*

[3]*Department of Biochemistry Biozentrum, University of Basel, 4056 Basel, Switzerland*

[4]*Novartis Pharma AG, 4002 Basel, Switzerland*

[5]*School of Biological Sciences University of Auckland Auckland 1001, New Zealand*

[6]*Department of Medicine School of Medicine, University of Auckland, Auckland 1001 New Zealand*

*Corresponding author

Pancreatic amyloid deposits, composed of the 37 amino acid residue peptide amylin, represent an integral part of type 2 diabetes mellitus pathology. Human amylin (hA) forms fibrils *in vitro* and is toxic to cultured pancreatic islet β-cells. In contrast, rat amylin (rA) which differs from hA by only six amino acid residues in the central region of the peptide, residues 18-29, does not form fibrils and is not cytotoxic. To elucidate the role of individual residues in fibril formation, we have generated a series of full-length rA variants and examined their ability to form fibrils *in vitro*. Single-residue substitutions with amino acids from corresponding positions of the hA sequence, i.e. R18H, L23F, or V26I, were sufficient to render rA competent for fibril formation albeit at a small yield. Combining two or three of these substitutions generally increased the ability to produce fibrils. Variant rA fibril morphologies were examined by negative stain electron microscopy and found to be similar to those generated by hA itself. Bulk assays, i.e. involving thioflavin-T fluorescence and sedimentation, showed that the amount of fibril formation was relatively small for these rA variants when compared to hA under the same conditions. Fibril growth was demonstrated by time-lapse atomic force microscopy, and MALDI-TOF mass spectrometry was used to verify that fibrils consisted of full-length peptide. Our observations confirm previous reports that the three proline residues play a dominant negative role in fibril formation. However, their presence is not sufficient to completely abolish the ability of rA to form fibrils, as each of the other three implicated residues (i.e. R18, L23 and V26) also has a dominant modulating effect.

© 2003 Elsevier Science Ltd. All rights reserved

Keywords: amylin; islet amyloid polypeptide (IAPP); amyloid; type 2 diabetes; proline residues

Introduction

Amylin is one of an increasing number of peptides with the ability to form amyloid deposits and cause disease.[1] It is the main constituent in the deposits that form in the islets of Langerhans of the pancreas in type 2 diabetes mellitus.[2,3] Amyloid deposits in this disease are associated with the depletion of islet β-cells, and are considered a hallmark of disease progression. Amylin,

a 37 amino acid residue protein (Figure 1) is produced in the islet β-cells and co-secreted with insulin. It belongs to a family of peptides (amylin, calcitonin, calcitonin-gene-related-peptide and adrenomedullin) sharing to varying extents metabolic functions in the control of nutrient assimilation, storage and disposal.[4–10]

The propensity of amyloid proteins to form fibrils *in vitro* parallels their cytotoxicity to cultured cells.[11–14] Amylin peptides derived from different species illustrate this point. Human amylin (hA) forms amyloid fibrils *in vitro* and is toxic to cultured pancreatic islet β-cells.[15] In contrast, the rat amylin isoform (rA), despite having 84% amino acid sequence similarity and only six amino acid changes compared to hA, does not form fibrils and is not cytotoxic (Figure 1). The

	18 23 26
Rat amylin	KCNTATCATQRLANFLV**R**SSNN**L**G**PV**L**PP**TNVGSNTY-CONH₂
Human amylin	KCNTATCATQRLANFLV**H**SSNN**F**G**AI**L**SS**TNVGSNTY-CONH₂

Figure 1. Primary sequences of rat and human amylin peptides. A disulphide bridge connects residues 2 and 7 in all of the peptides. The six residues that are different between rat and human amylin are enlarged.

identity of the cytotoxic substance, mature fibrillar species, elementary fibrillar intermediates, small oligomers, or monomers which have switched to an altered conformation, is still subject to controversy. Some evidence suggests that fibril intermediates or oligomers along the assembly pathway rather than the mature fibrils themselves are directly cytotoxic.[16,17]

Amyloid fibrils have been generally described as being several μm long and 8–10 nm in diameter with occasional twisting along the fibril axis.[1] Based on X-ray fibre diffraction studies a common structural model termed the "cross-β" model, was put forward in 1968.[18,19] This model describes a continuous array of β-strands forming extended twisted β-sheets stacking at approximately right angles to the fibril axis to yield so-called "elementary protofilaments". These, in turn, associate laterally to form the mature fibrils.[20] Molecular models of the elementary protofilament in various forms of amyloid have suggested that each molecule folds into two to four β-strands, and that these align to form an elongated β-sheet. Several of these may stack on top of each other to form the protofilament.[20–26] The number of protofilaments in mature fibrils may differ between amyloid proteins, and may be variable even for an individual protein as fibrils may be polymorphic.[27–34]

Peptide fragments corresponding to the central region of hA, i.e. amino acid residues 20–29 (SNNFGAILSS), 22–27 (NFGAIL), 23–27 (FGAIL) and 24–29 (GAILSS), can independently assemble into fibrils.[17,35–37] Their morphological appearance and ability to bind amyloid-specific dyes such as thioflavin-T (TFT) differs to varying extents from those formed by the full-length protein.[30]

The inability of rA to form fibrils is currently attributed to the three proline residues present in the central region of the 20–29 peptide, consistent with the general β-sheet disrupting effect of proline residues.[38–41] However, until now all three proline residues have not been simultaneously studied. Using the hA (20–29) peptide fragment, the proline residue at position 28 has been shown to greatly inhibit fibril formation, whereas the proline substitutions at positions 25 and 29 only slightly attenuate it.[38,39] Therefore it is conceivable that the inability of rA to form fibrils does not just reside in its three proline residues.

With this in mind, recent results demonstrating that the central region of hA is not the only amyloidogenic segment, are intriguing. Peptides spanning residues 8–20 (ATQRLANFLVHSS) and 30–37 (TNVGSNTY) also form fibrils.[37,42] This is consistent with the view that the amylin molecule is folded into three β-strands.[43,44] As the central strand contains the main sequence variations between hA and rA, it would appear that this segment, especially the presence or absence of proline residues, accounts for the differences in fibril formation competency and toxicity. The problem with this interpretation is that it is based on the behaviour of individual peptide fragments in
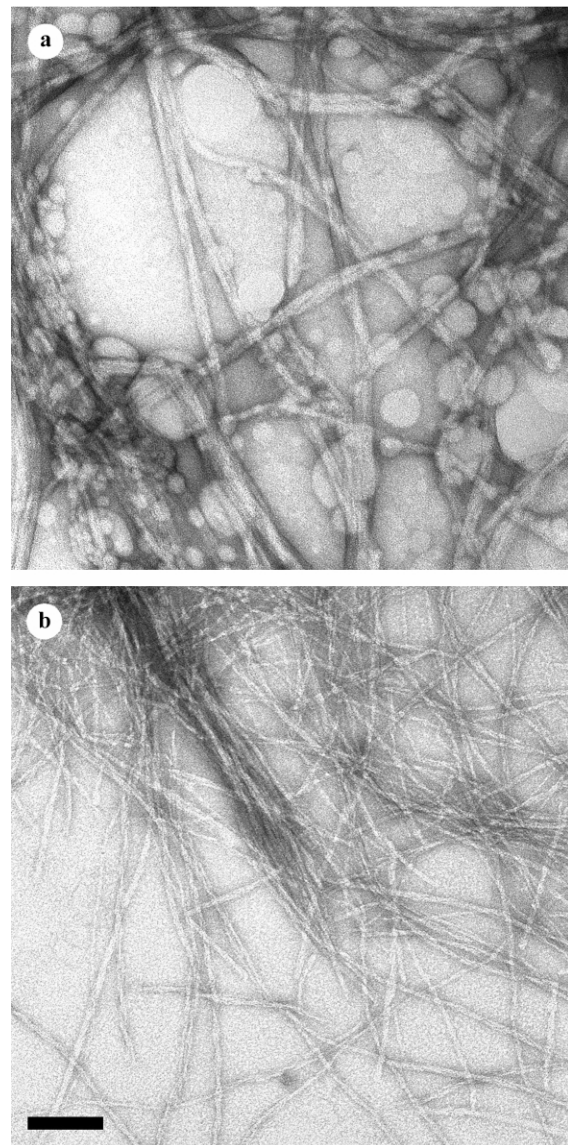
Figure 2. The three rA proline residues do not completely abolish fibril formation of a full-length hA peptide. Electron micrographs of negatively stained fibrils for (a) rA [R18H, L23F, V26I] and (b) hA. Scale bar represents 200 nm.

isolation rather than that of intact amylin molecules. If the flanking regions also contribute to β-sheet formation in the entire molecule, one could hypothesise that subtle changes in the central region might be sufficient to lend rA the ability to form fibrils.

Here we have tested this hypothesis by investigating fibril formation by full-length rA variants with one, two or all of the following point mutations: R18H, L23F andV26I. These residues were chosen, because in addition to the important proline substitutions at positions 25, 28 and 29, they distinguish rA from hA. Our results demonstrate that the ability of rA to form fibrils can indeed be achieved by substituting single amino acid residues with their hA counterparts. The propensity to form fibrils is further dramatically increased when the three proline residues are substituted with the corresponding amino acid residues of hA. These observations made with full-length rat amylin variants confirm the key role of the three proline residues, but for the first time demonstrate that their presence only decreases but does not fully abolish fibril formation by hA.

Results

Proline residues reduce but do not abolish fibril-forming competency
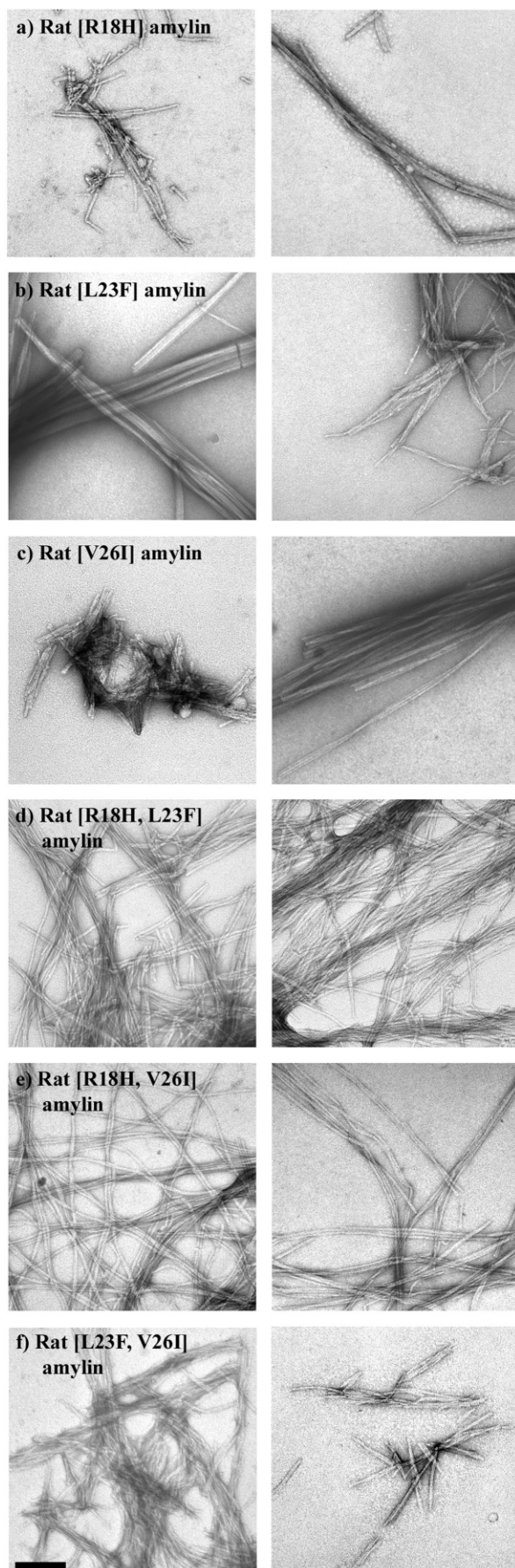
Previous experiments with the central segment of hA in isolation, showed that substitution of one or more of residues 25, 28 or 29 with proline (as they exist in rA) attenuates fibril formation.[38,39,45] We attempted to verify this finding by using a full-length rA variant which preserved the proline residues but substituted the other three rat-specific residues with their counterparts from the hA sequence, i.e. rA[R18H, L23F, V26I]. Stock solutions prepared by solubilising the lyophilised rA variant in MilliQ water, were diluted to 200 μM in phosphate-buffered saline (PBS) and incubated at room temperature. To our surprise, small amounts of fibrils were detected in these solutions by electron microscopy (EM) of negatively stained samples after seven days (Figure 2(a)). Globular structures of 50–200 nm in size were often seen in association with the fibrils, larger but possibly similar to those observed for β-amyloid (Aβ) (10–25 nm).[31] Compared to hA assayed under similar conditions which produced fibrils within ten minutes (Figure 2(b)), rA[R18H, L23F, V26I] fibril formation was considerably slower. A qualitative estimate of the amount of rA[R18H, L23F, V26I] fibrils present on the EM grid was less than 10% compared to those formed by hA under equivalent conditions. A more quantitative comparison of fibril formation was achieved using the TFT binding assay (Figure 3). Binding levels for rA[R18H, L23F, V26I] over a 20-day period were only marginally higher than for rA or buffer alone. In comparison, TFT binding
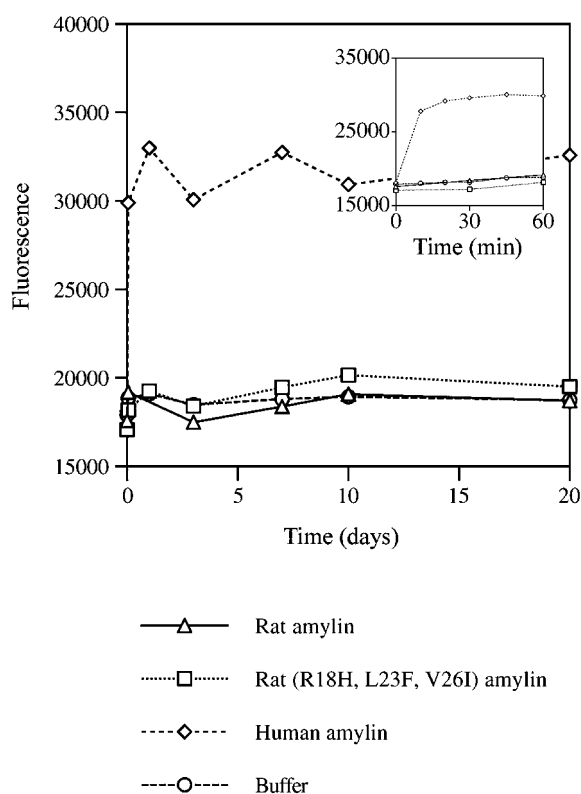
Figure 3. The kinetics of fibril formation for rA, rA [R18H, L23F, V26I], and hA as judged by TFT fluorescence. The TFT signal for rA [R18H, L23F, V26I] fibrils was only marginally higher than the background.
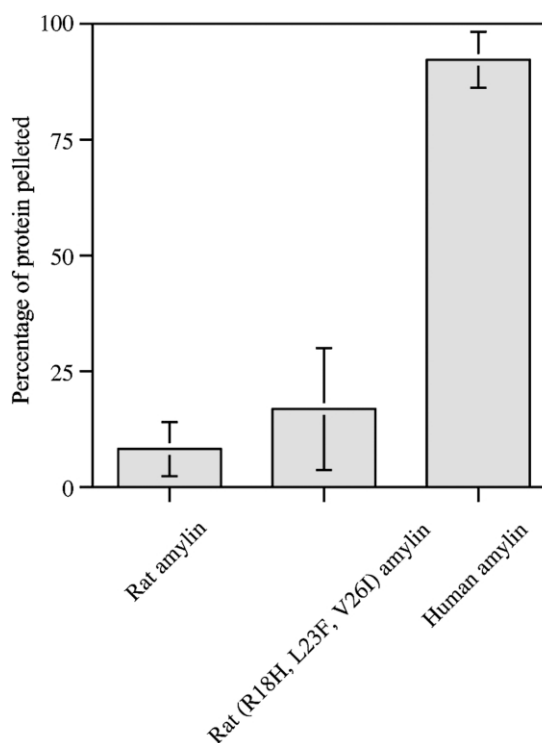
Figure 4. Quantification of rA, rA [R18H, L23F, V26I] and hA fibrils by sedimentation. The sedimentation assay does not detect the presence of the rA [R18H, L23F, V26I] fibrils.

Figure 5. rA peptides with one or two amino acid substitutions form fibrils. Electron micrographs of negatively stained fibrils for (a) rA [R18H], (b) rA [L23F], (c) rA [V26I], (d) rA [R18H, L23F], (e) rA [R18H, V26I] and (f) rA [L23F, V26I]. Scale bar represents 150 nm.

levels for hA reached near-maximum levels after just 45 minutes (Figure 3, inset). Given the low dye binding of rA[R18H, L23F, V26I] compared to hA, it is clear that proline residues dramatically reduce fibril formation. This was confirmed using a sedimentation assay that separates fibrils from unassembled molecules (Figure 4). hA and rA[R18H, L23F, V26I] pelleted 92% and 13% of their total protein, respectively. The percentage for rA[R18H, L23F, V26I] was only marginally higher than for sedimented rA (8%), which over the same time period did not produce any detectable fibrils by EM. Taken together, our results confirm that the three rA-specific proline residues significantly attenuate fibril formation. On the other hand, introducing the three hA-specific H18, F23 and I26 residues clearly promotes fibril-formation by rA.

Single amino acid substitutions render rA variants competent for fibril-formation

Having established that rA[R18H, L23F, V26I] gained the ability to form fibrils, we next examined which of the amino acid changes, R18H, L23F, or V26I, were critical for this gain of function. For this purpose, six rA variants were synthesised containing one or two of these substitutions. Stock solutions in MilliQ water were prepared from lyophilised peptides, diluted in PBS to a peptide concentration of 200 μM, and incubated at room temperature. Analysis by negative stain EM revealed that all six of the variant peptides formed fibrils albeit at different rates (Figure 5). rA[R18H, L23F] assembled the fastest, with fibrils detectable after three days incubation. rA[R18H, V26I] and rA[V26I] formed fibrils after two weeks incubation, and rA[L23F, V26I], rA[L23F] and rA[R18H] after three or four weeks. Higher-order coiling and lateral association of fibrils was often observed (see Figure 5), similar to but not identical to polymorphic forms previously described for hA fibrils.[29] Coiling with an axial cross-over spacing of approximately 60 nm was observed for rA[R18H, L23F], rA[R18H, V26I] and rA[L23F]. For comparison, hA forms coiled fibrils with distinct left-handed axial cross-over spacings of 25 nm, 50 nm and, occasionally, 37 nm.[29,30] None of the seven rA variants formed fibrils exhibiting these distinct hA morphologies.

From these results, it is evident that single amino acid substitutions are sufficient to render rA variants competent to form fibrils, albeit at significantly reduced amounts and much lower rates compared to hA. As was the case with rA [R18H,
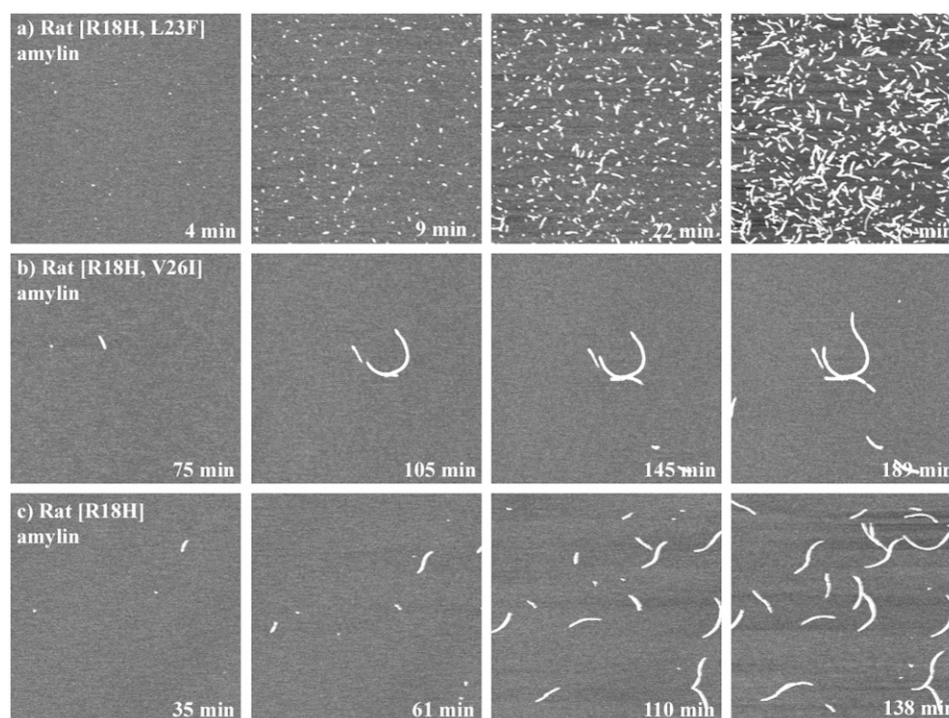
Figure 6. Time-lapse AFM for (a) rA [R18H, L23F], (b) rA [R18H, V26I], and (c) rA [R18H] at a concentration of 40 μM in PBS. Images are 2 μm × 2 μm as zoomed in from a 4 μm × 4 μm image.

L23F, V26I], none of the other six variant rA peptides exhibited TFT binding above background levels (data not shown). From our results it is evident that a negative TFT binding result does not necessarily mean the complete absence of fibrillar amyloid material. The absence of a TFT-positive signal may result from a low quantity of fibrils being present in the solution or a different ability of the amyloid-like fibrils to bind the TFT dye. This problem has been observed previously for both TFT and Congo Red dye binding[30,37,46] and has lead us to the conclusion that EM is a much more sensitive technique than TFT or congo red binding to detect the presence of amyloid-like fibrils.

The six rA variants with one or two amino acid substitutions were not C-terminally amidated. It could be argued that their ability to form fibrils is due to the absence of this modification. We believe this not to be true as preliminary results on amidated rA[R18H, L23F] and rA[R18H], using EM and time-lapse atomic force microscopy (AFM) reveal that these peptides do form fibrils with similar kinetics to their unamidated counterparts (data not shown).

Nucleation rates differ between rA variants

While EM proved to be a sensitive assay to detect fibril formation for the rA variants, it only provides a qualitative measure of the fibrilisation end-point. Therefore it was important to complement our static observation, i.e. that single amino acid substitutions rendered rA variants competent for fibril-formation, with a more kinetic assay. For

this purpose we chose time-lapse atomic force microscopy which, in contrast to the bulk methods such as EM, sedimentation or TFT binding, can directly visualise the growth of individual fibrils.[47] Moreover, this technique allowed us to directly compare the relative nucleation and elongation rates of the fibrils formed by the different rA variants. To achieve this, the fluid cell of the AFM was first filled with PBS and the mica surface examined for the presence of any contaminants. An equal volume of freshly diluted rA variant was then injected into the fluid cell and the growth of fibrils on the mica surface monitored by repeated scanning. At a concentration of 40 μM, hA formed fibrils on the mica surface within minutes, whereas no fibrils could be detected for wild-type rA even after nine hours. For the fastest fibril-forming rA variant, rA[R18H, L23F] as judged by EM, time-lapse AFM revealed nuclei after four minutes that grew into fibrils after 35 minutes (Figure 6(a)). AFM was also able to confirm fibril formation by rA[R18H, V26I] (Figure 6(b)) and rA[R18H] (Figure 6(c)). Their nucleation rates, however, were lower than that for rA[R18H, L23F] (Figure 6(b) and (c)), which is consistent with the qualitative assessment made by EM. On the other hand, fibrils formed by rA[R18H, V26I] and rA[R18H] were longer than those formed by rA[R18H, L23F] (see Figure 6). However, this difference is judged less significant, as fibril length was clearly concentration-dependent. For instance, when the concentration of rA[R18H, L23F] was decreased to 5–10 μM it could also form longer fibrils (data not shown).

Taken together, time-lapse AFM fully validated the observations made by negative stain EM, i.e. that single amino acid substitutions render rA competent to form fibrils. Moreover, this dynamic technique reveals subtle differences in the relative nucleation rates of the different rA variants.

Analysis of rA [R18H, L23F] fibrils by MALDI TOF mass spectrometry

Due to the recent findings that various segments of amylin can form fibrils in isolation [37,42], we needed to confirm that the fibrils made in our study did not result from the cleavage of the full-length peptide into smaller segments. We therefore analysed solubilised pellets from fresh and aged rA[R18H, L23F] solutions by MALDI TOF mass spectrometry. In both cases a major peak of approximately 3936 Da was obtained, corresponding to the size of the full-length peptide. In addition, peaks approximately 28 Da, 56 Da and 84 Da higher were found in the solubilised fibril sample, corresponding to formylated peptide. However, there was no evidence of cleaved peptides.

Discussion

Amylin has been known for some time to be the main component of the amyloid deposits that form in the pancreas of patients with type 2 diabetes. Yet the mechanism of amyloid formation by amylin and its role in disease progression have remained an enigma. To this end, *in vitro* assembly experiments with synthetic amylin or its variants are an important complement to eventually elucidate the mechanism of fibril formation *in vivo*. In this context, the observation that hA rapidly forms fibrils, whereas rA does not, is indeed interesting. Based on investigations using short amylin fragments corresponding to residues 20–29, the inability of rA to form fibrils has been attributed to the three proline residues present at positions 25, 28 and 29 in rA but not in hA. Our experiments confirm earlier reports that the proline residues of rA greatly reduce fibril formation by hA,[38,39,45] but they demonstrate for the first time that the three proline residues are not solely responsible for the inability of rA to form fibrils, as the rA variant rA [R18H, L23F, V26I] clearly exhibits the ability to form fibrils. In fact, one or any combination of the substitutions, R18H, L23F, V26I, renders the corresponding rA variants competent to form fibrils despite the presence of the three prolines, albeit with only small yields. It has been known since the 1970s that proline residues are powerful β-sheet disruptors.[40] What is less well known however, is that the proline residues strongly favour β-turns.[48,49] Evidently, β-turns appear to play an important role in stabilising tertiary structure, initiating folding and facilitating inter-

molecular recognition.[49,50] When considering the most recent model of the hA monomer folded into three β-strands, residue 28 is at the second position of a β-turn, i.e. representing the position in a β-turn at which proline residues are the most favourable.[43] Therefore proline 28 within the rat amylin variant peptides, may not actually break the β-strand but stabilise the β-turn, connecting β-strands two and three, thereby stabilising the β-sheet and hence promoting fibril formation. If indeed the proline residue at position 28 is involved in a β-turn, then the 20–29 fragment of the hA peptide would not serve as a good model for fibril formation by hA.

Our results are consistent with a recent model suggesting that hA folds into three β-strands forming an intramolecular β-sheet.[43] The central β-strand (i.e. 20–29) contains five out of the six residue differences between hA and rA, the sequence of the latter being disruptive to β-sheet formation. Our data strongly suggest that single amino acid substitutions in this region can restore, at least to some extent, the interactions with the flanking β-strands to yield a stable intramolecular β-sheet so that some fibril formation occurs.

Another key finding of our experiments is that the hA substitution R18H clearly has an enhancing effect on fibril formation. Previously, it was thought that in the case of hA this histidine does not participate in fibril formation.[36,42] This view is supported by the observation that both rA(1–20) and hA(1–20) fragments form fibrils with similar efficiency.[42] Studies with the Aβ peptide, however, have come to a different conclusion and regard the presence of the histidine residues at positions 13 and 14 important for fibrillogenesis.[51–54] The importance of the histidine residues in Aβ and hA may be due to the ability of such aromatic residues to stabilise β-sheets through π-stacking interactions within the protofilaments. Such a mechanism has recently been suggested by Gazit.[55] Other possible reasons that the histidine residue has an enhancing effect on fibrillogenesis is that it slightly increases the hydrophobicity as well as decreases the overall charge and alpha-helix propensity of the rat amylin peptide. All such mechanims have been recently shown to favour aggregation.[56–58]

Furthermore, F23 has been observed to be essential for fibril formation in experiments with the 22–27 hA peptide fragment (NFGAIL) in isolation.[35] This finding is consistent with our current experiments showing that the single L23F substitution in rA is sufficient to induce fibril formation of this variant. Other studies using hA segments in isolation also indicate that F23 may have a stabilising role in fibril formation.[17,37–39] More specifically, it was shown that the 24–27 hA fragment (GAIL) did not form fibrils, but that addition of F23 (FGAIL) did render this short peptide competent for fibril formation.[17] However, F23 became less important when longer fragments were used: for example, Nilsson observed that the

24–29 and 24–37 hA fragments formed fibrils in the absence of 23F.[37]

From the three variant rA peptides studied with just one amino acid change, rA [V26I] was the fastest to form fibrils. Consistent with this observation is the result obtained by Moriarty and colleagues who found that mutating I26 to proline had the most disruptive effect of any of the systematically substituted amino acid residue positions in the 20–29 hA segment.[38] In contrast, Westermark *et al.* found that mutating I26 to a valine had only a minor attenuating effect on the fibril-forming ability of the 20–29 hA fragment.[39]

In the present investigation, time-lapse AFM has been able to confirm the kinetics of fibril assembly, as judged by EM, for the variant amylin peptides. This is the first study showing that this technique is a powerful tool to directly compare the effect of single amino acid substitutions on a peptide's polymerisation kinetics, i.e. nucleation and elongation rates. Time-lapse AFM has the advantage that fibril growth can be imaged in real time in physiological buffer.[47,59] Here, we have been able to even identify and accumulate hA oligomers that eventually elongate into fibrils. This observation hints at the possibility that this technique may be able to distinguish between species that are on or off of the fibril forming pathway. This in turn, could be useful for identifying and characterising the critical nuclei necessary for amyloid fibril formation.

One other issue of using time-lapse AFM is that fibril growth is confined to a solid surface. At first glance, this may be seen as a disadvantage as it may be considered as an unphysiological condition, however, *in vivo* environments contain many surfaces, for example, the cell membrane, so this scenario may in fact be more physiological than anticipated. The confinement of the protein to a surface may lead to the stabilisation and/or accumulation of intermediates that are too short-lived in bulk solution to be depicted, as was the case for hA elementary protofilament.[47] This protofilament is only rarely seldom seen in bulk solution but can readily be accumulated on a solid support and imaged by AFM.

Taken together, our experiments with full-length rA variants complement observations made by others using shorter amylin segments. Substitutions in the latter were often reported to have all-or-nothing effects, for example, that the presence of proline residues abolishes fibril formation. We observed a more subtly graded effect in full-length rA variants, where fibril formation still occurred, albeit at reduced levels, even in the presence of three proline residues. Nevertheless, single amino acid substitutions were sufficient to render rA variants able to form fibrils. Overall, these observations suggest that the difference in fibril-forming competency between rA and hA is more finely tuned than previously thought, particularly when studied in full-length variants.

Materials and Methods

Peptide preparation

Lyophilised preparations of synthetic human amylin (lot numbers 514905, 538994) and rat amylin (lot number 542554) were purchased from Bachem (Torrence, CA). Variant amylin peptides were synthesised by Auspep (Australia). Purity was checked by HPLC and MALDI TOF mass spectrometry. Amylin stock solutions for fibril formation experiments (0.4 mM) and time-lapse AFM (3.2 mM) were prepared by weighing out the appropriate amount of lyophilised peptide and solubilising it in milliQ water or 1,1,1,3,3,3-hexafluoro-2-isopropanol (HFIP), respectively (Fluka). Peptide stock solutions were diluted to a concentration of 200 μM or 40 μM in PBS (10 mM Na_2HPO_4, 100 mM NaCl, pH 7.5) for fibril formation experiments and time-lapse AFM, respectively.

Transmission electron microscopy

Each solution was adsorbed to a glow-discharged carbon-coated collodion film on 400-mesh copper grids. The grids were blotted, washed three times with deionised water, and negatively stained with 0.75% (w/v) uranyl formate.[60] Grids were examined in an H-7000 Hitachi transmission electron microscope (Hitachi Ltd., Tokyo, Japan) operated at 100 kV. Images were recorded on Kodak electron image plate film at a nominal magnification of 50,000 $\times$.

Atomic force microscopy

For time-lapse AFM, PBS alone was scanned initially to check for the presence of any contaminants. The amylin peptide solutions were injected into the fluid cell to produce a final concentration of 40 μM (1.25% HFIP, PBS). Images were obtained with a Nanoscope IIIa multimode scanning probe workstation (Digital Instruments, Santa Barbara, CA) operating in tapping mode using a silicon nitride probe with a spring constant of 0.32 N/m. All imaging was performed at scan rates of 1.97 Hz using a cantilever drive frequency of approximately 9 kHz. All images were captured as 512 $\times$ 512 scans and were low-pass filtered.

Thioflavin-T assay

hA, rA, and rA [R18H, L23F, V26I] solutions (200 μM) were assayed for their ability to bind TFT dye over a period of 20 days. At each time-point amylin solutions (5 μl) were added to 10 mM Tris–HCl (pH 7.5) and 3 μM TFT. The fluorescence signal was measured (excitation wavelength 450 nm, emission wavelength 482 nm, slit widths set to 5 nm) on a Perkin–Elmer LS50B fluorimeter, adapted for 96-well microtitre plates.

Sedimentation assay

Aged solutions of hA (>seven days), rA, and rA [R18H, L23F, V26I] (2.5–3.5 months) were centrifuged at 100,000 rpm (Beckman TL-100) for 90 minutes. The supernatant was removed and the protein concentration was measured using the BCA protein assay (Pierce) and compared to the protein concentration of the original aged solution.

Mass spectrometry

Aged solutions of rA [R18H, L23F] (2.5–3.5 months) were centrifuged at 100,000 rpm (Beckman TL-100) for 90 minutes. The pellet was solubilised in 80% formic acid for one hour prior to sonication (3 × 30 seconds). The solubilised pellets or fresh peptide dissolved in water, were purified using C_{18} ZipTips (Millipore). MALDI-TOF analysis was performed on a Bruker REFLEX III mass spectrometer (Bruker Daltonik GmbH, Bremen, Germany). Purified peptide was mixed with 1 μl of matrix solution (10 mg/ml α-cyano-4-hydroxy-cinnamic acid (Aldrich) in 80% acetonitrile, 0.1% trifluoroacetic acid) and placed on the sample plate to dry. Calibration and mass measurements of the amylin peptides were carried out in the linear mode. Calibration of the instrument in the low molecular mass range was done using the monoisotopic masses of the adreno-corticotropic hormone (fragment 18–39; Fluka), substance P (Fluka), angiotensin (Fluka), and bombesin (Fluka).

References

1. Sipe, J. D. & Cohen, A. S. (2000). Review: history of the amyloid fibril. *J. Struct. Biol.* **130**, 88–98.
2. Clark, A., Cooper, G. J., Lewis, C. E., Morris, J. F., Willis, A. C., Reid, K. B. & Turner, R. C. (1987). Islet amyloid formed from diabetes-associated peptide may be pathogenic in type-2 diabetes. *Lancet*, **2**, 231–234.
3. Cooper, G. J., Willis, A. C., Clark, A., Turner, R. C., Sim, R. B. & Reid, K. B. (1987). Purification and characterization of a peptide from amyloid-rich pancreases of type 2 diabetic patients. *Proc. Natl Acad. Sci. USA*, **84**, 8628–8632.
4. Brain, S. D., Williams, T. J., Tippins, J. R., Morris, H. R. & MacIntyre, I. (1985). Calcitonin gene-related peptide is a potent vasodilator. *Nature*, **313**, 54–56.
5. Bauerfeind, P., Hof, R., Hof, A., Cucala, M., Siegrist, S., von Ritter, C., Fischer, J. A. & Blum, A. L. (1989). Effects of hCGRP I and II on gastric blood flow and acid secretion in anesthetized rabbits. *Am. J. Physiol.* **256**, G145–G149.
6. Cooper, G. J. (1994). Amylin compared with calcitonin gene-related peptide: structure, biology, and relevance to metabolic disease. *Endocr. Rev.* **15**, 163–201.
7. Cornish, J., Callon, K. E., King, A. R., Cooper, G. J. & Reid, I. R. (1998). Systemic administration of amylin increases bone mass, linear growth, and adiposity in adult male mice. *Am. J. Physiol.* **275**, E694–E699.
8. Hettiarachchi, M., Chalkley, S., Furler, S. M., Choong, Y. S., Heller, M., Cooper, G. J. & Kraegen, E. W. (1997). Rat amylin-(8–37) enhances insulin action and alters lipid metabolism in normal and insulin-resistant rats. *Am. J. Physiol.* **273**, E859–E867.
9. Leighton, B. & Cooper, G. J. (1988). Pancreatic amylin and calcitonin gene-related peptide cause resistance to insulin in skeletal muscle *in vitro. Nature*, **335**, 632–635.
10. Young, A. A., Cooper, G. J., Carlo, P., Rink, T. J. & Wang, M. W. (1993). Response to intravenous injections of amylin and glucagon in fasted, fed, and hypoglycemic rats. *Am. J. Physiol.* **264**, E943–E950.
11. DeArmond, S. J., McKinley, M. P., Barry, R. A., Braunfeld, M. B., McColloch, J. R. & Prusiner, S. B. (1985). Identification of prion amyloid filaments in scrapie-infected brain. *Cell*, **41**, 221–235.
12. Forloni, G., Angeretti, N., Chiesa, R., Monzani, E., Salmona, M., Bugiani, O. & Tagliavini, F. (1993). Neurotoxicity of a prion protein fragment. *Nature*, **362**, 543–546.
13. Lorenzo, A. & Yankner, B. A. (1994). Beta-amyloid neurotoxicity requires fibril formation and is inhibited by congo red. *Proc. Natl Acad. Sci. USA*, **91**, 12243–12247.
14. Schubert, D., Behl, C., Lesley, R., Brack, A., Dargusch, R., Sagara, Y. & Kimura, H. (1995). Amyloid peptides are toxic via a common oxidative mechanism. *Proc. Natl Acad. Sci. USA*, **92**, 1989–1993.
15. Lorenzo, A., Razzaboni, B., Weir, G. C. & Yankner, B. A. (1994). Pancreatic islet cell toxicity of amylin associated with type-2 diabetes mellitus. *Nature*, **368**, 756–760.
16. Janson, J., Ashley, R. H., Harrison, D., McIntyre, S. & Butler, P. C. (1999). The mechanism of islet amyloid polypeptide toxicity is membrane disruption by intermediate-sized toxic amyloid particles. *Diabetes*, **48**, 491–498.
17. Tenidis, K., Waldner, M., Bernhagen, J., Fischle, W., Bergmann, M., Weber, M. *et al.* (2000). Identification of a penta- and hexapeptide of islet amyloid polypeptide (IAPP) with amyloidogenic and cytotoxic properties. *J. Mol. Biol.* **295**, 1055–1071.
18. Eanes, E. D. & Glenner, G. G. X-r. (1968). ray diffraction studies on amyloid filaments. *J. Histochem. Cytochem.* **16**, 673–677.
19. Geddes, A. J., Parker, K. D., Atkins, E. D. & Beighton, E. (1968). "Cross-beta" conformation in proteins. *J. Mol. Biol.* **32**, 343–358.
20. Shirahama, T. & Cohen, A. S. (1967). High-resolution electron microscopic analysis of the amyloid fibril. *J. Cell. Biol.* **33**, 679–708.
21. Blake, C. & Serpell, L. (1996). Synchrotron X-ray studies suggest that the core of the transthyretin amyloid fibril is a continuous beta-sheet helix. *Structure*, **4**, 989–998.
22. Cardoso, I., Goldsbury, C. S., Muller, S. A., Olivieri, V., Wirtz, S., Damas, A. M. *et al.* (2002). Transthyretin fibrillogenesis entails the assembly of monomers: a molecular model for *in vitro* assembled transthyretin amyloid-like fibrils. *J. Mol. Biol.* **317**, 683–695.
23. Chaney, M. O., Webster, S. D., Kuo, Y. M. & Roher, A. E. (1998). Molecular modeling of the Abeta1–42 peptide from Alzheimer's disease. *Protein Eng.* **11**, 761–767.
24. Malinchik, S. B., Inouye, H., Szumowski, K. E. & Kirschner, D. A. (1998). Structural analysis of

Alzheimer's beta(1–40) amyloid: protofilament assembly of tubular fibrils. *Biophys. J.* **74**, 537–545.

25. Serpell, L. C., Sunde, M., Benson, M. D., Tennent, G. A., Pepys, M. B. & Fraser, P. E. (2000). The protofilament substructure of amyloid fibrils. *J. Mol. Biol.* **300**, 1033–1039.

26. Shirahama, T., Benson, M. D., Cohen, A. S. & Tanaka, A. (1973). Fibrillar assemblage of variable segments of immunoglobulin light chains: an electron microscopic study. *J. Immunol.* **110**, 21–30.

27. Bauer, H. H., Aebi, U., Haner, M., Hermann, R., Muller, M. & Merkle, H. P. (1995). Architecture and polymorphism of fibrillar supramolecular assemblies produced by *in vitro* aggregation of human calcitonin. *J. Struct. Biol.* **115**, 1–15.

28. Cohen, A. S., Shirahama, T. & Skinner, M. (1982). Electron microscopy of amyloid. In *Electron Microscopy of Protein* (Harrid, I., ed.), vol. 3, pp. 165–205, Academic Press, London.

29. Goldsbury, C. S., Cooper, G. J., Goldie, K. N., Muller, S. A., Saafi, E. L., Gruijters, W. T. *et al.* (1997). Polymorphic fibrillar assembly of human amylin. *J. Struct. Biol.* **119**, 17–27.

30. Goldsbury, C., Goldie, K., Pellaud, J., Seelig, J., Frey, P., Muller, S. A. *et al.* (2000). Amyloid fibril formation from full-length and fragments of amylin. *J. Struct. Biol.* **130**, 352–362.

31. Goldsbury, C. S., Wirtz, S., Muller, S. A., Sunderji, S., Wicki, P., Aebi, U. & Frey, P. (2000). Studies on the *in vitro* assembly of a beta 1–40: implications for the search for a beta fibril formation inhibitors. *J. Struct. Biol.* **130**, 217–231.

32. Harper, J. D., Wong, S. S., Lieber, C. M. & Lansbury, P. T. (1997). Observation of metastable Abeta amyloid protofibrils by atomic force microscopy. *Chem. Biol.* **4**, 119–125.

33. Kirschner, D. A., Inouye, H., Duffy, L. K., Sinclair, A., Lind, M. & Selkoe, D. J. (1987). Synthetic peptide homologous to beta protein from Alzheimer disease forms amyloid-like fibrils *in vitro*. *Proc. Natl Acad. Sci. USA*, **84**, 6953–6957.

34. Serpell, L. C., Sunde, M., Fraser, P. E., Luther, P. K., Morris, E. P., Sangren, O. *et al.* (1995). Examination of the structure of the transthyretin amyloid fibril by image reconstruction from electron micrographs. *J. Mol. Biol.* **254**, 113–118.

35. Azriel, R. & Gazit, E. (2001). Analysis of the minimal amyloid-forming fragment of the islet amyloid polypeptide. An experimental support for the key role of the phenylalanine residue in amyloid formation. *J. Biol. Chem.* **276**, 34156–34161.

36. Glenner, G. G., Eanes, E. D. & Wiley, C. A. (1988). Amyloid fibrils formed from a segment of the pancreatic islet amyloid protein. *Biochem. Biophys. Res. Commun.* **155**, 608–614.

37. Nilsson, M. R. & Raleigh, D. P. (1999). Analysis of amylin cleavage products provides new insights into the amyloidogenic region of human amylin. *J. Mol. Biol.* **294**, 1375–1385.

38. Moriarty, D. F. & Raleigh, D. P. (1999). Effects of sequential proline substitutions on amyloid formation by human amylin 20–29. *Biochemistry*, **38**, 1811–1818.

39. Westermark, P., Engstrom, U., Johnson, K. H., Westermark, G. T. & Betsholtz, C. (1990). Islet amyloid polypeptide: pinpointing amino acid residues linked to amyloid fibril formation. *Proc. Natl Acad. Sci. USA*, **87**, 5036–5040.

40. Chou, P. Y. & Fasman, G. D. (1978). Empirical predictions of protein conformation. *Annu. Rev. Biochem.* **47**, 251–276.

41. Minor, D. L., Jr & Kim, P. S. (1994). Measurement of the beta-sheet-forming propensities of amino acids. *Nature*, **367**, 660–663.

42. Jaikaran, E. T., Higham, C. E., Serpell, L. C., Zurdo, J., Gross, M., Clark, A. & Fraser, P. E. (2001). Identification of a novel human islet amyloid polypeptide beta-sheet domain and factors influencing fibrillogenesis. *J. Mol. Biol.* **308**, 515–525.

43. Jaikaran, E. T. & Clark, A. (2001). Islet amyloid and type 2 diabetes: from molecular misfolding to islet pathophysiology. *Biochim. Biophys. Acta*, **1537**, 179–203.

44. Padrick, S. B. & Miranker, A. D. (2001). Islet amyloid polypeptide: identification of long-range contacts and local order on the fibrillogenesis pathway. *J. Mol. Biol.* **308**, 783–794.

45. Betsholtz, C., Christmanson, L., Engstrom, U., Rorsman, F., Jordan, K., O'Brien, T. D. *et al.* (1990). Structure of cat islet amyloid polypeptide and identification of amino acid residues of potential significance for islet amyloid formation. *Diabetes*, **39**, 118–122.

46. LeVine, H. (1995). Thioflavin T interations with amyloid beta-sheet structures. *Amyloid: Int. J. Exp. Clin. Invest.* **2**, 1–6.

47. Goldsbury, C., Kistler, J., Aebi, U., Arvinte, T. & Cooper, G. J. (1999). Watching amyloid fibrils grow by time-lapse atomic force microscopy. *J. Mol. Biol.* **285**, 33–39.

48. Hutchinson, E. G. & Thornton, J. M. (1994). A revised set of potentials for beta-turn formation in proteins. *Protein Sci.* **3**, 2207–2216.

49. Richardson, J. S. (1981). The anatomy and taxonomy of protein structure. *Advan. Protein Chem.* **34**, 167–339.

50. Rose, G. D., Gierasch, L. M. & Smith, J. A. (1985). Turns in peptides and proteins. *Advan. Protein Chem.* **37**, 1–109.

51. Curtain, C. C., Ali, F., Volitakis, I., Cherny, R. A., Norton, R. S., Beyreuther, K. *et al.* (2001). Alzheimer's disease amyloid-beta binds copper and zinc to generate an allosterically ordered membrane-penetrating structure containing superoxide dismutase-like subunits. *J. Biol. Chem.* **276**, 20466–20473.

52. Fraser, P. E., McLachlan, D. R., Surewicz, W. K., Mizzen, C. A., Snow, A. D., Nguyen, J. T. & Kirschner, D. A. (1994). Conformation and fibrillogenesis of Alzheimer A beta peptides with selected substitution of charged residues. *J. Mol. Biol.* **244**, 64–73.

53. Huang, X., Atwood, C. S., Moir, R. D., Hartshorn, M. A., Vonsattel, J. P., Tanzi, R. E. & Bush, A. I. (1997). Zinc-induced Alzheimer's Abeta1–40 aggregation is mediated by conformational factors. *J. Biol. Chem.* **272**, 26464–26470.

54. Yang, D. S., McLaurin, J., Qin, K., Westaway, D. & Fraser, P. E. (2000). Examining the zinc binding site of the amyloid-beta peptide. *Eur. J. Biochem.* **267**, 6692–6698.

55. Gazit, E. (2002). A possible role for pi-stacking in the self-assembly of amyloid fibrils. *Faseb J.* **16**, 77–83.

56. Chiti, F., Calamai, M., Taddei, N., Stefani, M., Ramponi, G. & Dobson, C. M. (2002). Studies of the aggregation of mutant proteins *in vitro* provide insights into the genetics of amyloid diseases. *Proc. Natl Acad. Sci. USA*.

57. Chiti, F., Taddei, N., Baroni, F., Capanni, C., Stefani, M., Ramponi, G. & Dobson, C. M. (2002). Kinetic partitioning of protein folding and aggregation. *Nature Struct. Biol.* **9**, 137–143.

58. Taddei, N., Capanni, C., Chiti, F., Stefani, M., Dobson, C. M. & Ramponi, G. (2001). Folding and aggregation are selectively influenced by the conformational preferences of the alpha-helices of muscle acylphosphatase. *J. Biol. Chem.* **276**, 37149–37154.

59. Stolz, M., Stoffler, D., Aebi, U. & Goldsbury, C. (2000). Monitoring biomolecular interactions by time-lapse atomic force microscopy. *J. Struct. Biol.* **131**, 171–180.

60. Bremer, A., Haner, M. & Aebi, U. (1997). Negative staining. In *Cell Biology: A Laboratory Hand Book* (Celis, J. E., ed.), 2nd edit., vol. 3, pp. 277–284, Academic Press, New York.

Edited by W. Baumeister